

Synthesis Characterization and study of Dielectric Properties of Conducting Co-polymer of PANIPPY/Y₂O₃ Nanocomposites

T. K. Vishnuvardhan, V. R. Kulkarni, C. Basavaraja and Shahshidhar

Department of chemistry, Acharya Institute of Technology, Bangalore-90

Department of chemistry, Central college, Bangalore-01

Department of Chemistry & IFM, Inje University, Kimhae-621 749, South Korea

Department of Chemistry, SDM College of Engineering and Technology, Dharwad-580 002,

e-mail : Vishnuvardhan@acharya.ac.in, bubvrk@gmail.com, chitragarabasavaraja@gmail.com and nshashidharreddy@gmail.com

Abstract : Nanocomposite materials have emerged as alternatives to overcome limitations of microcomposites and monolithics, while posing preparation challenges related to the control of elemental composition and stoichiometry in the nanocluster phase. Conducting polymer composites of PolyanilinePolypyrrole/yttrium oxide (PANIPPY/Y₂O₃) composites were prepared by insitu polymerization of aniline and pyrrole with varied amounts of Y₂O₃. The Content of Y₂O₃ is varied in weight percentages of 10%, 20%, 30%, 40%, and 50%. Synthesized composites are characterized by infrared (IR) and X-ray diffraction techniques (XRD). The surface morphology of the composites is investigated by scanning electron microscopy (SEM) Tunneling electron microscopy(TEM). Thermal analysis of the synthesized composites are also discussed. Electrical conductivity of the compressed pellets depends on the concentration of Y₂O₃ in PANIPPY. The transport property is discussed for frequency dependent ac conductivity, dielectric constant and dielectric loss reveals that the Y₂O₃ concentration in PaniPPY is responsible. Cole-Cole plot of the PaniPPY/Y₂O₃ composites is used to predict the relaxation behavior.

Key words : PANIPPY/Y₂O₃ compoistes, Dielectric constant, copolymer composites, Cole-Cole plots relaxation time.

1. INTRODUCTION

Conducting polymers and its blends exhibit a wide range of novel electrochemical and chemical properties that has led to their use in a diverse array of applications insensors [1-2]. Polyaniline, and polypyrrole is one of the most promising candidates for industrial application of conducting polymers. It is formed via simple chemical or electrochemical oxidation of aniline and pyrrole. There is large number of reports explains the polyaniline and its metal oxide[3-5] composites and polypyrrol and its metal oxide[6-8] composites with systematic characterization of conductivity dielectric and its applicational studies may be found. Conducting polyaniline blends and composites are prepared mostly via the chemical oxidation route, although electrochemical synthesis is also employed in some cases [9-10]. Electrochemical method of synthesis of PANIPPY copolymer synthesized by Bekir et al., [11] with different electrolyte and in different medium like water and acetonitrile had reported in 1998. Synthesis characterization of panippy copolymer composites are also synthesized by electrochemical method and coated over the steel and carbon rods had been reported by Rajagopal anetal [12-14].

Synthesis of polyaniline and its blends [15-16] also found

in the literature and polypyrrole and its blend in the literature are maximum [17-19].

In order to determine the composition, size, structural and thermal properties of the PANIPPY/Y₂O₃ nanocomposite structural investigations using X-ray, IR and morphological studies by SEM and TEM techniques were carried out and the results are presented here. The electrical properties of the nanocomposites are also discussed in this paper.

2. EXPERIMENTAL

2.1 Materials and methods

We procured pyrrole from Fluka, Aniline from S.d.fine chemicals. Pyrrole monomer is distilled by fusing with KOH and then collected at 131 °C. Fraction obtained is collected and kept in a closed vessel. It darkens on exposure to light so it is stored at 4 °C in the absence of light. Aniline is also distilled and collected at 182-185 °C. We procured anhydrous iron (III) chloride from Fischer (AR-grade), Yttrium oxide (Y₂O₃-) procured from S.d.fine chemicals.

The infrared spectra of polymer composites and pure oxide powders were recorded on a Perkin Elmer FTIR

spectrophotometer model 1600 series in the range 350 cm^{-1} to 4000 cm^{-1} in KBr medium at room temperature. The X-ray powder diffraction patterns of the above synthesized polymer composites were recorded on Philips X-ray diffractometer using CuK_α ($\lambda = 1.5406\text{ \AA}$). The shape, size, distribution of the grains for the above prepared polymer and its composites powder samples, microstructure of the polymer composites have been examined using Phillips XL30 ESEM scanning electron microscopy and Leica-440 Cambridge Stereoscan. For most of the samples 10, 5K and 2.5K magnification are used for clear vision of the morphology.

The particle size and morphology of the representative samples from the above prepared PaniPPy Y_2O_3 composite nanoparticles, the nature of interaction between the conducting and insulating components were determined using high resolution transmission electron microscopic studies (HRTEM; JEM 2010). The isopropyl alcohol is used as a solvent for the preparation of grid with applied voltage of 4000 KV.

TGA of PaniPPy/oxide composites were recorded over a temperature range of 26°C to 1200°C in nitrogen atmosphere using a STA 409C thermal analyzer, to analyze the degradation pattern of polymer composites. Simultaneously, Differential Thermal Analysis (DTA) data was also recorded. Reference material used in the TGA/DTA is Alumina with heating rate of temperature is 5 K/min.

Frequency dependent electrical measurements are made by using the Hawlett-Packard impedance analyzer HP 4194A in the frequency range 10^2 - 10^6 Hz at room temperature and applied voltage maintained at 2V.

2.2 Synthesis of Pani-PPy co-polymer and Pani-PPy/oxide composites

0.02 mole of pyrrole and 0.02 moles of aniline are added drop wise to an 100ml of solution containing 0.06 mole of FeCl_3 with continuous stirring. Monomer to monomer ratio is maintained at 1:1 and monomer to oxidant also kept constant i.e., 1:3 to observe the effect of oxide on the polymerization of copolymer. The reaction mixture was stirred continuously at 0°C . The black precipitate of the PANIPPY copolymer formed was collected by filtration and thoroughly washed with distilled water, until the filtrate became colourless. Any unreacted pyrrole/aniline in the copolymer was removed by washing, the precipitate with methanol and the copolymer was dried under vacuum at room temperature. [20,21,22]

During the synthesis of the copolymer, varied amount of Y_2O_3 powder ($n = 10, 20, 30, 40,$ and 50% by weight) is added with continuous stirring. The use of 1:1 ratio (w/w) of monomer is for polymerization of aniline and pyrrole for synthesis of copolymers is maintained. PPy composite coating samples were prepared with a relatively proportional, molar ratio of 1:3 is maintained. The reaction mixture was agitated continuously for 3 hrs, during this process, the solution was always kept at 0°C . The black precipitate of the PANIPPY/ Y_2O_3 composites formed was collected by filtration and thoroughly washed with distilled water, until the filtrate became colourless. Any unreacted pyrrole in the composite was removed by washing the precipitate with methanol and the composite was dried under vacuum at room temperature.

3. RESULTS AND DISCUSSION

The FTIR spectra of FPPZ (FPPZ) show intense characteristic peaks indicate the formation of doped copolymer. Which are further confirmed from the Bekiret.al^[1] reports. XRD of the copolymer shows the one broad peak indicating the homogeneously mixing of the Pani and PPy and more crystalline than the pure PPy (FPZ) or pure Pani from the literature. Further, SEM and TEM image confirms the agglomerated particles of irregular spherical shape of copolymers.

3.1 FTIR

Figure 1(a) - (e) show the above significant absorption bands for FPP10YZ, FPP30YZ, FPP50YZ composites and Y_2O_3 respectively. The peaks are not clear or ill defined, indicates the aromatic ring vibrations of pyrrole and aniline molecules are in different planes so some of the stretching frequencies are shifted. That is shifting from 1550 cm^{-1} to 1577 cm^{-1} after the formation of copolymer which is a characteristic peak for pyrrole ring vibrations. Similarly for 1204, 1050, 935 cm^{-1} their corresponding frequencies in pure PPy is 1180, 1046 and 918 cm^{-1} . This indicates that PPy and Pani interact to form copolymer or substituted product is formed. Further oxide peaks are also observed in the composites around 350 cm^{-1} shows presence of oxide in the composite but there is no chemical interaction. There may be a weak interaction between oxide and the copolymer. There is slight shifting of peaks in the composites may be due to the difference in chain length after the addition of oxide.

3.2 XRD

Figure 2 (a), (b) and (c) shows the XRD patterns of pure FPPZ FPP10YZ and FPP30YZ samples respectively.

They indicate the amorphous nature of PaniPPy/Y₂O₃ composite samples with varying weights of Y₂O₃ composites. Presence of sharp peaks reveals the some degree of crystallinity in the sample. With these two representative samples crystallinity increases as the oxide content in the composite increases. As there is a broad peak still indicates after the formation of composites also amorphous nature still existing. Some of the Y₂O₃ peaks are not defined indicates that copolymer is cover the oxide planes so x-rays are not sufficiently scattered those plane.

3.3 SEM

Figure 3(a) - (d) shows 10K magnification SEM images of the FPPZ, FPP10YZ, FPP30YZ and FPP50YZ samples prepared in FeCl₃ medium. Morphology of the growing surface is influenced by the type of oxide and supporting medium. The Y₂O₃ particles are covered by copolymer of PaniPPy having irregular shape forming compact and globular arrangement. Approximate particle size of the FPPZ, FPP10YZ, FPP30YZ and FPP50YZ samples are 200 nm, 250 nm and 253 nm and 256 nm respectively.

3.4 TEM

Figure 4. Shows the TEM of the representative FPP30YZ composite. The particles appear to be capped one over the other to form chain and finally forms cluster covers the oxide particles. Average grain size is 100 nm.

The FTIR spectra of FPPnYZ show the characteristic peaks for the FPPZ and that of Yttrium oxide indicating the doped copolymer-oxide composite. Variation in the characteristic copolymer peaks may be due to the different extent of copolymerization in presence of oxide in the copolymer. FTIR peaks are not clear for FPPnYZ composites, but the presence of oxide also seen in the composites. This may be due to interference of one polymer with the other polymer along with the oxide or copolymers are homogeneously distributed with the oxide particles. But here polymerization of polyaniline and polypyrrole may need more oxidant so oxidation may be insufficient or addition of oxide may also affect the copolymerization leading to ill defined peaks. In case of FPPnYZ samples comparatively well defined peaks indicates that in presence of Y₂O₃ copolymerization is not affected much so leading to well defined FTIR spectra.

The XRD peaks of FPPnYZ are almost similar with that of FPPZ samples. The addition of oxide increases in the copolymer composites as crystallinity increases with decrease in broad peak for the copolymer, single broad peak indicating the homogeneous mixing of polyaniline

and polypyrrole. These peak intensity decreases with increase in oxide indicating the crystallinity of FPPnYZ. Further morphological (SEM and TEM images) features like particles dispersed and forming the cluster with the oxide is confirmed.

3.5 Thermal analysis

Figure 5 shows TG curve of FPPZ and FPP10YZ sample. Steep TG curve of FPP10YZ composite contain two stages of degradation from room temperature to 550 °C. First stage of degradation starts at room temperature to 150 °C and second degradation curve is from 150 to 550 °C. The onset temperature and T_{max} for the second stage degradation of the composite is 310 and 550 °C. Total weight loss is during the degradation is about 90%. This indicates that the composite is more crystalline and less stable than the FPPZ sample.

Figure 6 indicates the DSC curves for FPPZ and FPP50YZ composite. Curve for pure Pani in the pure Pani-PPy is obtained at around 73 °C but in case of Pani in PaniPPy/Y₂O₃ composites appear at 63.32 °C with broad dip but sharp T_g for FPPnYZ appears at 82.192 °C may be due to PPY it also consists of one more dip at 428.516 °C which indicate the overlapping of the oxide decomposition with melting or decomposition of the polymer.

3.6 Electrical conductivity

Figure 7 shows the frequency dependent conductivity of the PaniPPy/Y₂O₃ composites. Frequency independent region is quite shorter than that for the pure FPPZ sample i.e. 10²-10⁴ Hz. (except for FPP30YZ sample for which hardly there is any frequency independent region). Table 1 shows the room temperature conductivity at 100 Hz frequency and crossover frequency values of FPPnYZ sample.

Figure 8 indicates the conductivity as a function of percentage of yttrium oxide in FPPnYZ samples at 100 Hz frequency. First two oxide composites show lower conductivity than the PaniPPy. FPP30YZ composite show from initial frequency itself continuous and rapid increase in the conductivity values as the frequency is increased.

Table 1 : Conductivity values at 100 Hz frequency and cross over frequency of FPPnYZ composites.

Composites	Conductivity(S/cm)	Crossover frequency (Hz)
FPPZ	1.948×10^{-7}	1×10^5
FPP10YZ	2.501×10^{-8}	1×10^5
FPP20YZ	1.4792×10^{-7}	3×10^5
FPP30YZ	2.7592×10^{-7}	—
FPP40YZ	2.9525×10^{-7}	1×10^5
FPP50YZ	7.061×10^{-8}	1×10^5

PANIPPY/oxide composites: The addition of one more monomer (Pani) during the synthesis, i.e., oxidation, leading to a restriction for the growing polymer chain may due to two reasons a) competition in the growing polymer chains or b) the side chain formation. Further, addition of oxide may act as impurity so that growing polymer may further be restricted. Hence, oxide particles are not completely covered by the polymer as observed from SEM and TEM results. Oxide particles are partially covered by the polymers so oxide-oxide interaction may be more leading to lowering of conductivity.

3.7 Dielectric constant and Dielectric Loss

Figure 9 and 10 presents the frequency dependent dielectric constant and dielectric loss for the FPPnYZ composites. Inset of the figure show Dielectric constant and dielectric loss for pure FPPZ. Frequency dependent dielectric loss for FPP30YZ sample show slightly different from the usual curve. Frequency dependent region of the dielectric constant and dielectric loss region is 10^5 and 10^7 Hz respectively.

Table 2 indicates the dielectric constant and dielectric loss (at 100 Hz) for FPPnYZ samples. Figure 11 indicate the dielectric constant and dielectric loss as a function of percentage of Yttria in FPPnYZ composite samples. It indicates that FPP30YZ composite show highest dielectric constant of 3454 and its dielectric loss value is 1.44. Highest dielectric loss value found for FPP40YZ sample.

Composites	Dielectric constant	Dielectric loss
FPPZ	686	5.12
FPP10YZ	149	3.03
FPP20YZ	376	3.36
FPP30YZ	3454	1.44
FPP40YZ	663	7.97
FPP50YZ	543	5.10
Pure Y_2O_3	5.08	0.653

3.8 Relaxation Behaviour

In practice, the Cole-Cole plots are often not exactly semicircular but are distorted to varying degrees. Similarly, the peaks in the imaginary impedance Z'' are not symmetric Debye peaks but are often broadened asymmetrically. The traditional approach to describing such distorted peaks is to regard them as the superposition of an appropriate number of individual Debye peaks, each occurring at different frequency^{4,5}. This introduces the

concept of a distribution of relaxation times. In Cole-Cole plot representation. Cole-Cole plot units used for the X-coordinate should be equal to the Y-coordinate or if the plots become so small, then half the X-axis coordinate is equated to the Y-coordinate and some time if plots are half the semicircular then such plots can be fitted by a polynomial of second order for further calculation of the relaxation time⁶⁻¹⁰.

Relaxation time (T) is a characteristic time that determines the sluggishness of the dipole response to an applied field. It is the mean time for the dipole to lose its alignment with the field due to its random interactions with the other molecules through molecular collisions, lattice vibrations and so forth^{8,9}.

Figure 12 depicts the Cole-Cole plots of the FPPnYZ samples. Inset of the figure shows the Cole-Cole plot of the FPPZ sample. All these samples show almost semicircular curves which is distributed to some extent. Table 3 indicates the relaxation time for FPPnYZ samples. Figure 13 indicates relaxation time as a function of weight percentage of Yttrium oxide in FPPnYZ composites. For FPP10YZ composite show high relaxation time that of others show lower relaxation time.

Table 3 : Relaxation time of FPPnYZ and FPPnYZ composites.

Composites	τ Sec
FPPZ	5.308×10^{-5}
FPP10YZ	1.592×10^{-4}
FPP20YZ	7.962×10^{-5}
FPP30YZ	7.962×10^{-6}
FPP40YZ	1.769×10^{-5}
FPP50YZ	5.308×10^{-5}

4. CONCLUSION

PaniPPycopolymer were synthesized and encapsulate the yttria particles. Is ensured by FTIR and XRD surface morphology of the pani ppy Y_2O_3 composites are irregular shape and having particle size around 200-250nm. Polymer chain capped one over the other over the metal oxide. DSC and TG shows the thermal stability of the composites. Panippy copolymer oxide composites also shows the conductivity range almost 10^{-8} to 10^{-7} s/cm at room temperature. Composites also shows the dielectric constants in the range of 150 to 3500 FPP30YZ shows the highest dielectric constant and lowest dielectric loss

value. Cole cole plots for the all the copolymer composites shows the semi circle and lowest relaxation is also shown to the FPP30 YZ composite.

5. REFERENCES

1. TW Lewis, MR Smyth, GG Wallace. *Analyst* 124 1999, 213.
2. A Mirmohseni, AOLadegaragoze. *J Appl Polym Sci* 85, 2002, 2772
3. Narsimha Parvatikar, Shilpa Jain, Syed Khasim, M. Revansiddappa, S.V. Bhoraskar, M.V.N. Ambika Prasad *Sensors and Actuators B* 114 (2006) 599–603
4. N. N. Mallikarjuna, S. K. Manohar, P. V. Kulkarni, A. Venkataraman, T. M. Aminabhavi *Journal of Applied Polymer Science*, Vol. 97, **2005** 1868–1874.
5. Kaushik Mallick, Michael J Witcomb, Michael S Scurrrell, Andre M Strydom, *Gold Bulletin* 41, **2008**/3.
6. T.K. Vishnuvardhan, V.R. Kulkarni, C. Basavaraja and S.C. Raghavendra *Bull. Mater. Sci.*, 29, (1), **2006**, 77–83.
7. C. Basavaraja, Young Min Choi, Hyun Tae Park, Do Sung Huh, Jae Wook Lee, M. Revanasiddappa, S.C. Raghavendra, S. Khasim, and T. K. Vishnuvardhan *Bull. Korean Chem. Soc.*, 28,**2007**, 7.
8. S C Raghavendra, S Khasim, M Revanasiddappa, M V N Ambikaprasad and A B Kulkarni, *Bull.Mat.Sci.*, 26, **2003**, 733.
9. Soares DAW, AAA de Queiroz. *Macromol Symp*;170, **2001** : 221
10. M Karakisla, M Sacak, U. J Akbulut *Appl Polym Sci*; 59(9): **1996**, 1347.
11. Bekir sari and Muzaffer Talu, *Synthetic Metals* 94, **1998**, 221-227
12. Ramakrishnan Rajagopalan, Jude O. Iroh *Electrochimica Acta* 46, **2001**, 2443–2455.
13. Ramakrishnan Rajagopalan, Jude O. Iroh *Electrochimica Acta* 47, **2002**, 1847/1855.
14. Ramakrishnan Rajagopalan, Jude O. Iroh, *Applied Surface Science* 218, **2003**, 58–6.
15. Suprakas Sinha Ray, Mukul Biswas *Synthetic Metals* 108, **2000**, 231–236.
16. Akira Kitani, Kousukesathoguchi, Kenji Iwai and sutoroIto. *Synthetic Metals* 102, **1999**, 1171-72.
17. L.C. Costa, F. Henry, M.A. Valente, S.K. Mendiratta, A.S. Sombra *European Polymer Journal*, 38, **2002**, 1495–1499.
18. S. Bhattacharyya and S. K. Saha T. K. Mandal, B. M. Mandal, and D. Chakravorty K. Goswam, *Journal of Applied Physics*, 10, **2001**.89
19. Rupali Gangopadhyay and Amitabha De *J. Mater. Chem.* 12, **2002**, 3591–3598
20. Tian B and Zerbi G, *J Chem. Phys.*, **92**(6), 1990, 3886.
21. Fatih K`OLEL_I, Meltem D and Yasemin ARSLAN *Turk J Chem* 24 **2000**, 333- 341.
22. Amit Bhattacharya and Amithabha De, *Prog.Solid St. Chem.* 24, **1996**,141.

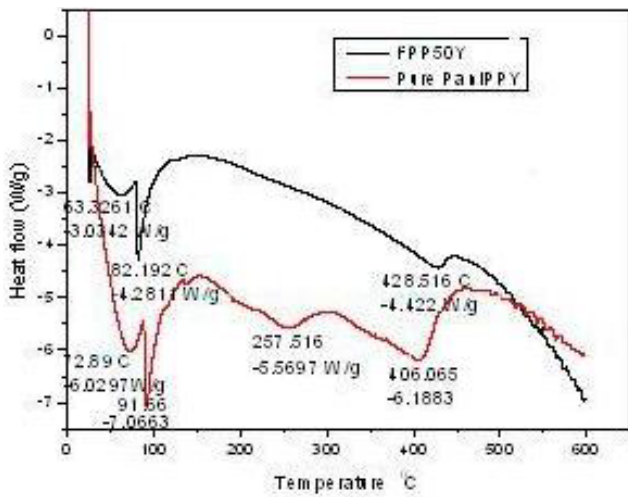


Figure - 6.

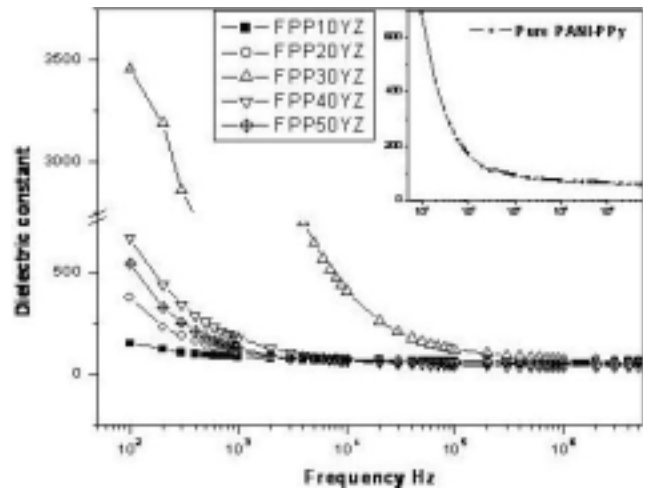


Figure - 9.

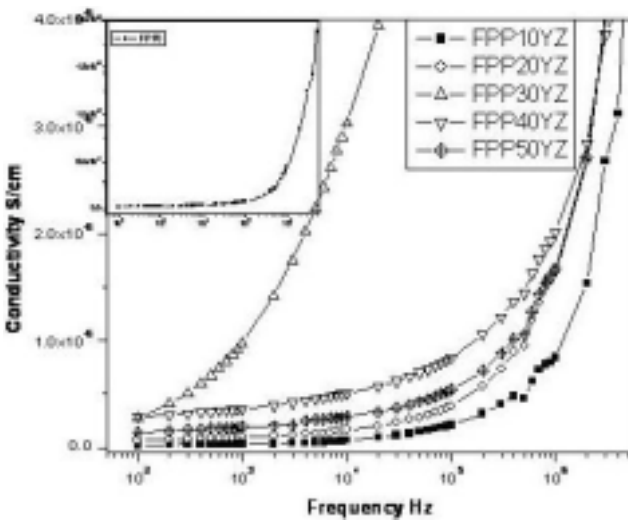


Figure - 7.

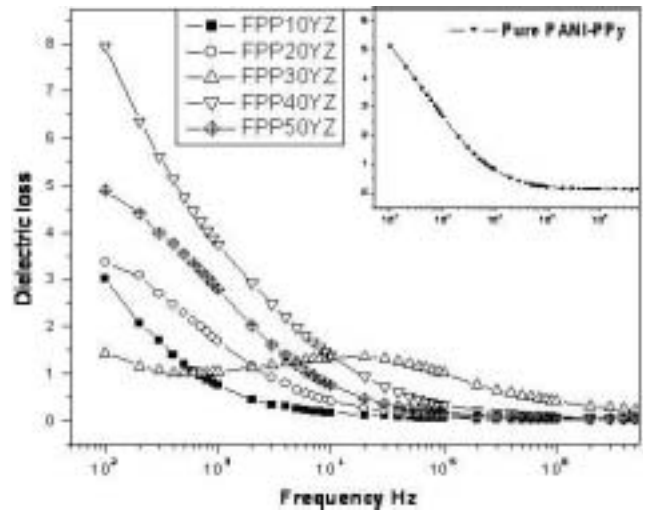


Figure - 10.

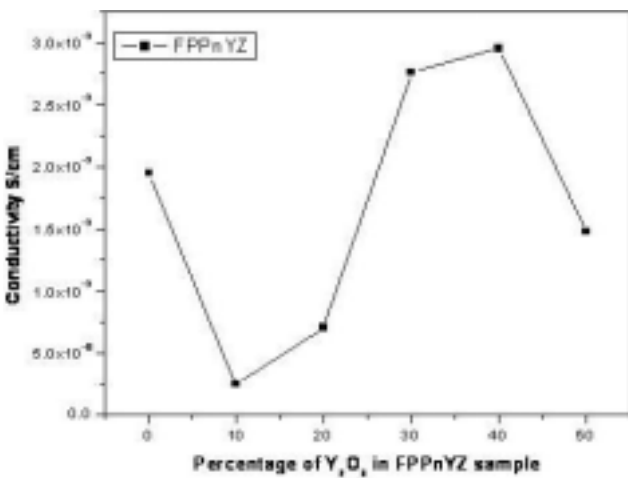


Figure - 8.

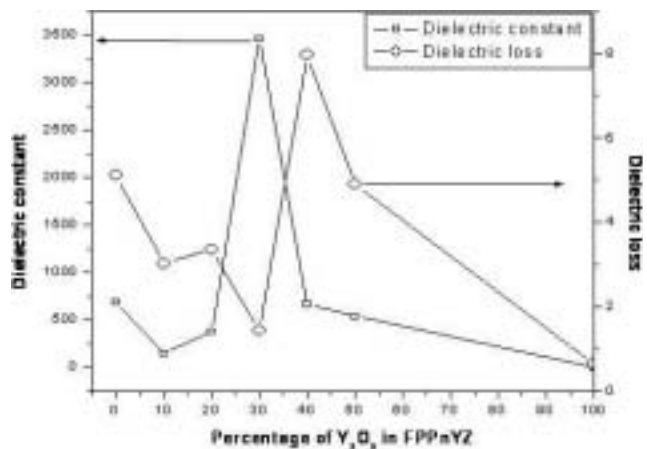


Figure - 11.

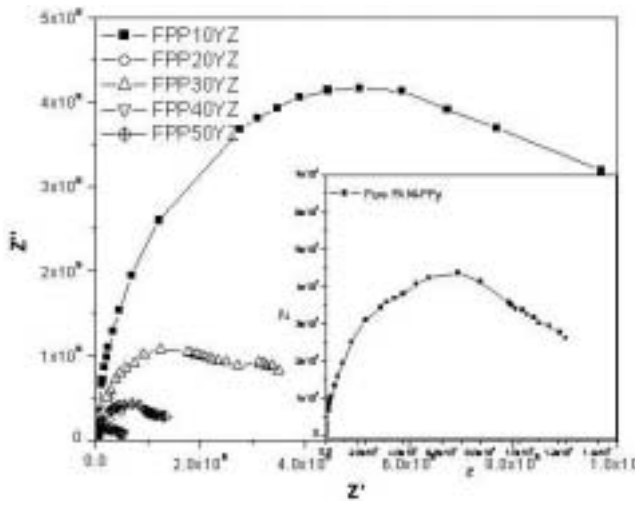


Figure - 12.

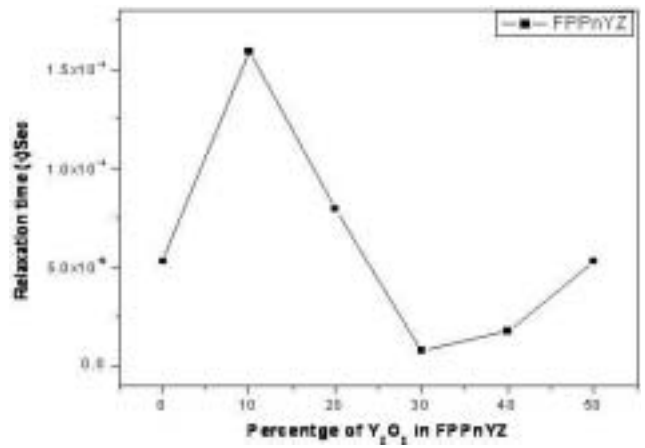


Figure - 13.